SUPPLEMENTARY INFORMATION

Neoadjuvant PD-L1 versus PD-L1 plus CTLA-4 Blockade for Patients with Malignant Pleural Mesothelioma

Hyun-Sung Lee, M.D., Ph.D.[1], Hee-Jin Jang, M.D., Ph.D.[1], Maheshwari Ramineni, M.D. [2], Daniel Y. Wang, M.D. [3], Daniela Ramos, B.S.[1], Jong Min Choi, Ph.D.[1], Taylor Splawn, M.P.H.[1], Monica Espinoza, B.S.[1], Michelle Almarez, B.S.[1], Leandria Hosey, B.S.[1], Eunji Jo, M.S.[4], Susan Hilsenbeck, Ph.D.[4], Christopher I. Amos, Ph.D.[5], R. Taylor Ripley, M.D.[6], Bryan M. Burt, M.D.[1,*]

Supplementary Table 1. Representativeness of Study Participants.

Cancer type/subtype/stage/condition	Resectable malignant pleural mesothelioma (MPM) /all histologies
Considerations related to	
Sex	MPM is 4-5 times more prevalent in males and may be less biologically aggressive in females. Furthermore, differential patterns of gene expression have been associated with sex in MPM.
Age	The risk of MPM increases with age. MPM can occur in young people (even children), but it's rare in people under age 45. About 2 out of 3 people with MPM are 65 or older. The average age for a MPM diagnosis is 72.
Race/ethnicity	MPM is more common in White and Hispanic people than in Asian American or African American people.
Geography	Although MPM is a fairly rare disease (0.6% of annual cancer deaths), its worldwide incidence and mortality are projected to rise due to continued asbestos exposure from manufacturing, accidents, and abatement. Approximately 3,500 patients are diagnosed with MPM in the U.S. annually, and its incidence is expected to peak around 85,000 deaths in the U.S. alone in the 2020s-50s. Texas has the 4th highest death rate from MPM in the nation. The public health hazard in the U.S. persists in incidents ranging from asbestos-abatement projects to the 9/11/2001 destruction of the World Trade Center.
Other considerations	MPM is an aggressive lethal, malignancy. Few effective treatments exist for MPM and its 5-year mortality is greater than 90%. The most common etiology of MPM is industrial/environmental exposure to asbestos (~80%).
Overall representativeness of this study	The mean age at the time of enrollment of this trial is around 64 years old. Our study population was limited to our institution's main site in Houston, TX. The MPM distribution of ethnic and racial categories mirrors the demographic data in our center, i.e. approximately 90% White subjects (including 5% Hispanic subjects), 5% Black or African American subjects, and 3% Asian subjects. In aggregate, the other minority groups account for 2% of our patient population.

Supplementary Table 2. Preoperative adverse events, defined as AEs observed after ICB and before surgery.

	Durva (N=9)			Durva+Treme (N=11)			Any
Grade	**1**	**2**	**3**	**1**	**2**	**3**	**Any**
Acute kidney injury	0	0	0	1	0	0	1
Alanine aminotransferase increased	1	0	0	1	0	0	2
Alkaline phosphatase increased	1	0	0	0	0	0	1
Anemia	2	0	0	3	1	0	6
Anorexia	0	0	1	0	0	0	1
Back pain	1	1	0	0	0	0	2
Chest wall pain	1	0	0	1	0	0	2
Chronic kidney disease	0	1	0	0	0	0	1
Cough	0	0	0	1	0	0	1
Dizziness	0	0	0	1	0	0	1
Dyspepsia	1	0	0	0	0	0	1
Dyspnea	2	0	1	0	0	1	4
Edema limbs	0	0	1	0	0	0	1
Fatigue	1	0	1	3	0	0	5
Fever	0	0	0	0	1	0	1
Hematuria	0	0	0	3	0	0	3
Hepatitis	0	0	0	0	0	1	1
Hyperglycemia	3	0	0	4	0	2	9
Hyperkalemia	0	0	0	1	0	0	1
Hypermagnesemia	1	0	0	0	0	0	1
Hypoalbuminemia	0	0	0	1	0	0	1
Hypocalcemia	0	0	0	1	0	0	1
Hypomagnesemia	0	0	0	2	0	0	2
Hyponatremia	0	0	0	1	0	0	1
Hypothyroidism	0	0	0	1	0	0	1
Leukocytosis	1	0	0	1	1	0	3
Lymphocyte count decreased	0	0	0	1	0	0	1
Myocardial Infarction	0	0	0	0	0	1	1
Nausea	1	1	0	1	0	0	3
Pain	0	0	0	1	0	0	1
Pleural effusion	0	0	0	0	1	0	1
Prolonged aPTT	1	0	0	0	0	0	1
Rash acneiform	0	0	0	0	0	1	1

Salivary duct inflammation	0	0	0	1	0	0	1
Sinus Bradycardia	1	0	0	0	0	0	1
Sore throat	0	0	0	1	0	0	1
Total AEs	18	4	4	31	4	6	60
Total participants	6	3	1	6	2	3	14
Total participants (%)	66.7	33.3	11.1	54.5	18.2	27.3	70

AEs, adverse events; aPTT, activated partial thromboplastin time.

Supplementary Table 3. Postoperative 30-day adverse events (AEs) observed after surgery.

Arm	No ICB (N=4)					Durvalumab (N=8)					Durva + Treme (N=9)					Any
Grade	**1**	**2**	**3**	**4**	**5**	**1**	**2**	**3**	**4**	**5**	**1**	**2**	**3**	**4**	**5**	**Any**
Abdominal pain	1	0	0	0	0	0	0	0	0	0	0	0	0	0	0	1
Acidosis	0	0	0	0	0	1	0	1	0	0	0	0	0	0	0	2
Acute coronary syndrome	0	0	0	0	0	0	0	0	1	0	0	0	0	0	0	1
Acute kidney injury	1	0	1	0	0	0	0	0	1	0	0	0	0	0	0	3
Alanine aminotransferase increased	0	1	0	0	0	1	0	0	1	0	0	1	0	0	0	4
Alkaline phosphatase increased	2	0	0	0	0	0	1	0	0	0	0	0	0	0	0	3
Anemia	3	0	1	1	0	4	0	1	0	0	2	0	0	0	0	12
Anorexia	2	1	0	0	0	0	0	0	0	0	0	0	0	0	0	3
Anxiety	1	1	0	0	0	0	0	0	0	0	0	0	0	0	0	2
aPTT prolonged	0	0	0	0	0	1	0	0	0	0	0	0	0	0	0	1
Aspartate aminotransferase increased	1	0	0	0	0	2	0	0	1	0	0	0	0	0	0	4
Atrial fibrillation	0	1	0	0	0	0	1	0	0	0	0	0	0	0	0	2
Blood bilirubin increased	0	0	0	0	0	1	1	0	0	0	0	0	0	0	0	2
Breast pain	0	0	0	0	0	1	0	0	0	0	0	0	0	0	0	1
Chest wall pain	1	0	0	0	0	0	1	0	0	0	0	1	0	0	0	3
Chronic kidney disease	0	0	0	0	0	0	0	0	0	0	0	1	0	0	0	1
Constipation	1	0	0	0	0	2	1	0	0	0	1	0	0	0	0	5
Cough	1	0	0	0	0	0	0	0	0	0	0	0	0	0	0	1
Creatinine increased	0	0	0	0	0	2	1	0	0	0	0	0	0	0	0	3
Death	0	0	0	0	0	0	0	0	0	1	0	0	0	0	0	1
Delirium	0	0	0	0	0	0	0	0	0	0	1	0	0	0	0	1
Dysphagia	1	0	0	0	0	0	0	0	0	0	0	0	0	0	0	1
Dyspnea	1	0	0	0	0	1	0	0	0	0	0	0	0	0	0	2
Edema limbs	0	0	0	0	0	1	1	0	0	0	0	1	0	0	0	3
Fall injury	0	0	1	0	0	0	0	0	0	0	0	0	0	0	0	1
Fatigue	2	1	0	0	0	0	0	0	0	0	0	0	0	0	0	3
Fever	0	0	0	0	0	1	0	0	0	0	0	0	0	0	0	1
Fibrinogen decreased	0	0	0	0	0	1	0	0	0	0	0	0	0	0	0	1
Heart failure	0	0	0	1	0	0	0	0	1	0	0	0	0	0	0	2
Hyperglycemia	3	1	0	0	0	3	1	0	0	0	0	0	0	0	0	8
Hyperkalemia	0	0	0	0	0	0	0	0	0	0	0	1	0	0	0	1
Hypernatremia	1	0	0	0	0	1	0	0	0	0	0	0	0	0	0	2

Hypoalbuminemia	0	0	0	0	0	1	0	0	0	0	0	0	0	0	0	1
Hypocalcemia	0	0	0	0	0	2	0	0	0	0	1	0	0	0	0	3
Hyponatremia	0	0	0	0	0	1	0	0	0	0	1	0	0	0	0	2
Hypotension	2	0	1	0	0	0	1	1	0	0	0	0	0	0	0	5
Hypoxia	0	0	0	0	0	0	0	0	0	0	0	1	0	0	0	1
Insomnia	1	0	0	0	0	0	0	0	0	0	0	0	0	0	0	1
Mucosal infection	1	0	0	0	0	0	0	0	0	0	0	0	0	0	0	1
Multi-organ failure	0	0	0	0	0	0	0	0	1	0	0	0	0	0	0	1
Nausea	1	0	0	0	0	1	1	0	0	0	0	0	0	0	0	3
Neck pain	1	0	0	0	0	0	0	0	0	0	0	0	0	0	0	1
Paresthesia	1	0	0	0	0	0	0	0	0	0	0	0	0	0	0	1
Platelet count decreased	0	0	0	0	0	1	1	0	0	0	0	0	0	0	0	2
Pleural effusion	1	0	0	0	0	0	0	0	0	0	0	0	0	0	0	1
Respiratory failure	0	0	0	0	0	0	0	0	1	0	0	0	0	0	0	1
Restlessness	1	0	0	0	0	0	0	0	0	0	0	0	0	0	0	1
Skin infection	0	1	0	0	0	0	0	0	0	0	0	0	0	0	0	1
Syncope	0	0	1	0	0	0	0	0	0	0	0	0	0	0	0	1
Urine output decreased	0	1	0	0	0	0	0	0	0	0	0	0	0	0	0	1
Ventricular tachycardia	0	1	0	0	0	1	0	0	0	0	1	0	0	0	0	3
Weight gain	0	0	0	0	0	0	0	0	0	0	0	1	0	0	0	1
Weight loss	1	0	0	0	0	0	0	0	0	0	0	0	0	0	0	1
White blood cell decreased	0	1	0	0	0	1	0	0	0	0	0	0	0	0	0	2
Total AEs	31	10	5	2	0	31	11	3	7	1	7	7	0	0	0	115
Total participants	4	4	3	1	0	6	4	1	1	1	4	4	0	0	0	16
Total participants (%)	100	100	75	25	0	75	50	25	25	25	44.4	44.4	0	0	0	76.2

AEs, adverse events; aPTT, activated partial thromboplastin time; LFT, liver function test.

Supplementary Table 4. Univariable analysis of variables associated with pathologic response and overall survival following neoadjuvant ICB (N=17).

Variable	Pathologic Response		Overall Survival	
	Odds ratio (95% CIs)	P value	Hazard ratio (95% CIs)	P value
Age		1.0		0.519
≤65 years old	1		1	
>65 years old	1.143 (0.141-9.289)		1.561 (0.403-6.055)	
Gender		1.000		0.532
Female	1		1	
Male	1.876 (0.150-23.26)		1.642 (0.347-7.752)	
Asbestos exposure		0.889		0.499
No	1		1	
Yes	0.857 (0.098-7.510)		0.643 (0.179-2.313)	
Clinical stage		0.600		0.194
I	1		1	
II	0.350 (0.029-4.153)		2.332 (0.649-8.381)	
Histology		0.644		0.417
Epithelioid	1		1	
Non-epithelioid	1.75 (0.233-13.159)		1.614 (0.482-5.819)	
Tumor PD-L1		**0.035**		0.181
≤5%	1		1	
>5%	2.747 (1.258-6.024)		2.900 (0.609-13.812)	
SUVmax	0.814 (0.557-1.190)	0.288	1.042 (0.964-1.127)	0.296
Neoadjuvant ICB		1.000		**0.041**
Monotherapy	1		1	
Combination therapy	0.833 (0.114-6.111)		0.247 (0.065-0.940)	
irAEs		0.333		0.594
No	1		1	
Yes	4.167 (0.358-48.44)		1.448 (0.371-5.652)	
Pretreatment CD8 (%)	0.865 (0.671-1.117)	0.267	1.031 (0.906-1.173)	0.648
Posttreatment CD8 (%)	0.981 (0.814-1.183)	0.841	1.003 (0.887-1.135)	0.959
Pretreatment Treg (%)	1.322 (0.739-2.363)	0.346	0.810 (0.543-1.208)	0.301
Posttreatment Treg (%)	1.189 (0.791-1.788)	0.405	1.091 (0.914-1.301)	0.335
Pretreatment CD8/Treg ratio	0.463 (0.174-1.229)	0.122	1.021 (0.902-1.155)	0.744
Posttreatment CD8/Treg ratio	0.968 (0.876-1.069)	0.519	0.990 (0.932-1.053)	0.759
Pretreatment TLS density>1/μm²	2.000 (1.112-4.452)	**0.044**	0.354 (0.044-2.844)	0.329
Posttreatment TLS	12.788 (1.315-	**0.028**	1.659 (0.440-6.253)	0.455

density>1/µm²	124.396)			
Pathologic response (viable tumor<80%) No Yes	-	-	 1 1.425 (0.400-5.072)	0.585
Residual viable tumor (%)	-	-	1.002 (0.984-1.024)	0.802
ypStage 0 or 1 Others	-	-	 1 1.072 (0.300-3.829)	0.914
Operative procedure Others EPP	-	-	 1 6.315 (1.259-31.671)	**0.025**
Intraoperative transfusion No Yes	-	-	 1 0.879 (0.247-3.131)	0.842
HIOC No Yes	-	-	 1 1.823 (0.522-6.364)	0.347
Macroscopic complete resection No Yes	-	-	 1 0.401 (0.113-1.417)	0.156
Adjuvant chemotherapy No Yes	-	-	 1 0.253 (0.062-1.028)	**0.055**
Adjuvant radiotherapy No Yes	-	-	 1 1.107 (0.139-8.827)	0.923

EPP, extrapleural pneumonectomy; HIOC, heated intraoperative chemotherapy; irAEs, immunotherapy-related adverse events; TLS, tertiary lymphoid structures.

Supplementary Table 5. IMC antibody panel relevant to Figure 1 and Figure 3.

No	PRODUCT	TAG	TARGET	CLONE	reactivity	PRODUCT #
1	CD38 141Pr	141Pr	CD38	EPR4106	human	3141018D
2	CD19 142Nd	142Nd	CD19	6OMP31	cross	3142014D
3	Vimentin 143Nd	143Nd	Vimentin	D21H3	cross	3143027D
4	TGFB1 144Nd	144Nd	TGFB1	310-390 aa, C-terminal	human	LS-B14346
5	CTLA-4 145Nd	145Nd	CTLA-4		human	A2001
6	CD16 146Nd	146Nd	CD16	EPR16784	human	3146020D
7	CD163 147Sm	147Sm	CD163	EDHu-1	human	3147021D
8	Pan-Keratin 148Nd	148Nd	Pan-Keratin	C11	human	3148020D
9	CD11b 149Sm	149Sm	CD11b	EPR1344	human/mouse	3149028D
10	CD278 150Nd	150Nd	CD278	SP98	human	ab236226
11	CD31 151Eu	151Eu	CD31	EPR3094	human	3151025D
12	CD45 152Sm	152Sm	CD45	CD45-2B11	human	3152016D
13	CD44 153Eu	153Eu	CD44	IM7	human/mouse	3153029D
14	CD11c 154Sm	154Sm	CD11c	Polyclonal	human	3154025D
15	FoxP3 155Gd	155Gd	FoxP3	236A/E7	human	3155016D
16	CD4 156Gd	156Gd	CD4	EPR6855	human	3156033D
17	E-Cadherin 158Gd	158Gd	E-Cadherin	24E10	cross	3158029D
18	CD68 159Tb	159Tb	CD68	KP1	human	3159035D
19	Vista 160Gd	160Gd	Vista	D1L2G	human	3160025D
20	CD20 161Dy	161Dy	CD20	H1	human	3161029D
21	CD8a 162Dy	162Dy	CD8a	C8/144B	human	3162034D
22	PD-L1 163Dy	163Dy	PD-L1		human	conjugated
23	c-Myc p67 164Dy	164Dy	C-Myc p67	9E10	human	3164025D
24	PD-1 165Ho	165Ho	PD-1		human	conjugated
25	CD45RA 166Er	166Er	CD45RA	HI100	human	3166028D
26	Granzyme B 167Er	167Er	Granzyme B	EPR20129-217	human	3167021D
27	Ki-67 168Er	168Er	Ki-67	B56	cross	3168022D
28	IL-10 169Er	169Er	IL-10		human	conjugated
29	CD3 170Er	170Er	CD3	Polyclonal, C-Terminal	human	3170019D
30	CD27 171Yb	171Yb	CD27	EPR8569	human	3171024D
31	CX3CR1 172Yb	172Yb	CX3CR1	2A9-1	human	3172017B
32	CD45RO 173Yb	173Yb	CD45RO	UCHL1	human	3173016D
33	HLA-DR 174Yb	174Yb	HLA-DR	YE2/36 HLK	human	3174023D
34	CD86 175Lu	175Lu	CD86	BU63	human/mouse	ab213044
35	Lysozyme 176Yb	176Yb	Lyz	EPR2994(2)	human/mouse	ab185129
36	Intercalator-Ir	191Ir	nucleus			SKU 201192B

Supplementary Table 6. CyTOF antibody panel for PBMC, relevant to Figure 4.

No	PRODUCT	TAG	TARGET	CLONE	reactivity	Source	PRODUCT #
1	CD45 89Y	89Y	CD45	HI30	human	DVS-Fluidigm	3089003B
2	CD57 115In	115In	CD57	HCD57	human	BioLegend	322325
3	IdU I127	127I	S-phase		DNA	Sigma	I7125-5G
4	CD56 139La (NCAM16.2)	139La	CD56	NCAM16.2	human	BD	559043
5	HLA ABC 141Pr	141Pr	HLA ABC	W6/32	human	DVS-Fluidigm	3141010B
6	CD19 142Nd	142Nd	CD19	HIB19	human	DVS-Fluidigm	3142001B
7	CD5 143Nd	143Nd	CD5	UCHT2	human	DVS-Fluidigm	3143007B
8	CD11b 144Nd	144Nd	CD11b	ICRF44	human	DVS-Fluidigm	3144001B
9	CD4 145Nd	145Nd	CD4	RPA-T4	human	DVS-Fluidigm	3145001B
10	CD8a 146Nd	146Nd	CD8a	RPA-T8	human	DVS-Fluidigm	3146001B
11	CD20 147Sm	147Sm	CD20	2H7	human	DVS-Fluidigm	3147001B
12	CD27 148Nd	148Nd	CD27	LG.3A10	human/mouse	BioLegend	124202
13	CD45RO 149Sm	149Sm	CD45RO	UCHL1	human	DVS-Fluidigm	3149001B
14	CD11c 150Nd	150Nd	CD11c	Bu15	human	BioLegend	337221
15	CD123 151Eu	151Eu	CD123	6H6	human	DVS-Fluidigm	3151001B
16	CD21 152Sm	152Sm	CD21	BL13	human	DVS-Fluidigm	3152010B
17	CD272 153Eu	153Eu	CD272, BTLA	J168-540	human	BD	558485(custom)
18	CD28 154Sm	154Sm	CD28	CD28.2	human	BioLegend	302937
19	CD278 155Gd	155Gd	CD278, ICOS	C398.4A	human/mouse	BioLegend	313502
20	CD86 156Gd	156Gd	CD86	IT2.2	human	DVS-Fluidigm	3156008B
21	CD25 158Gd	158Gd	CD25	BC96	human	BioLegend	302602
22	CCR7(CD197) 159Tb	159Tb	CD197, CCR7	G043H7	human	DVS-Fluidigm	3159003A
23	CD279 (PD-1) 160Gd	160Gd	CD279, PD-1	PD1.3.1.3	human	Miltenyi	130-096-168
24	CD152 (CTLA-4) 161Dy	161Dy	CD152	14D3	human	DVS-Fluidigm	3161004B
25	FoxP3 162Dy	162Dy	FoxP3	259D/C7	human	DVS-Fluidigm	3162024A
26	CD45RA 163Dy	163Dy	CD45RA	HI100	human	BioLegend	304102
27	TIM-3/Fc 164Dy	164Dy	TIM-3/Fc		human	R&D	2365-TM-050
28	CD40 165Ho	165Ho	CD40	5C3	human	DVS-Fluidigm	3165005B
29	Arginase-1 166Er	166Er	Arginase-1	Polyclonal	human/mouse	DVS-Fluidigm	3166023B
30	CD38 167Er	167Er	CD38	HIT2	human	DVS-Fluidigm	3167001B
31	CD154 (CD40L) 168Er	168Er	CD154, CD40L	24-31	human	DVS-Fluidigm	3168006B
32	CD161 169Tm	169Tm	CD161	HP-3G10	human	BioLegend	339902
33	CD3 170Er	170Er	CD3	UCHT1	human	DVS-Fluidigm	3170001B
34	CD68 171Yb	171Yb	CD68	Y1/82A	human	DVS-Fluidigm	3171011B

35	CD274 (PD-L1) 172Yb	172Yb	CD274, PD-L1	29E.2A3	human	BioLegend	329702
36	CD14 173Yb	173Yb	CD14	HCD14	human	BioLegend	325602
37	HLA-DR 174Yb	174Yb	HLA-DR	L243	human	BioLegend	307602
38	LAG-3 175Lu	175Lu	CD223/LAG-3	11C3C65	human	DVS-Fluidigm	3175033B
39	Ki67 176Yb	176Yb	Ki67	A019D5	human	BioLegend	350502
40	CD16 209Bi	209Bi	CD16	3G8	human	DVS-Fluidigm	3209002B
41	Intercalator-Ir	191Ir	nucleus			DVS-Fluidigm	SKU 201192B
42	Cisplatin-198Pt	198Pt	Cell viability			DVS-Fluidigm	SKU 201198

Supplementary Table 7. CyTOF antibody panel for PBMC, BMMC, and tumor-infiltrating immune cells, relevant to Figure 4 and Figure 5.

No	PRODUCT	TAG	TARGET	CLONE	reactivity	Source	PRODUCT #
1	CD57 115In	115Ln	CD57	HCD57	human	BioLegend	322325
2	IdU I127	127I	IdU127		DNA	Sigma	I7125-5G
3	CD56 139La (NCAM16.2)	139La	CD56	NCAM16.2	human	BD	559043
4	EpCAM 141Pr	141Pr	CD326(EpCAM)	9C4	human	DVS-Fluidigm	3141006B
5	CD19 142Nd	142Nd	CD19	HIB19	human	BioLegend	302202
6	CD117 143Nd	143Nd	CD117	104D2	human	DVS-Fluidigm	3143001B
7	CD11b 144Nd	144Nd	CD11b	ICRF44	human	DVS-Fluidigm	3144001B
8	CD4 145Nd	145Nd	CD4	RPA-T4	human	BioLegend	300502
9	CD8a 146Nd	146Nd	CD8a	RPA-T8	human	DVS-Fluidigm	3146001B
10	CD278 147Sm	147Sm	CD278(ICOS)	C398.4A	human/mouse	BioLegend	313502
11	CD27 148Nd	148Nd	CD27	LG.3A10	human	Biolegend	3147001B
12	CD200 149Sm	149Sm	CD200	OX-104	human	DVS-Fluidigm	3149007B
13	CD86 150Nd	150Nd	CD86	IT2.2	human	DVS-Fluidigm	3150020B
14	CD123 151Eu	151Eu	CD123	6H6	human	DVS-Fluidigm	3151001B
15	TCRgd 152Sm	152Sm	TCRgd	11F2	human	DVS-Fluidigm	3152008B
16	Pan-CK 153Eu	153Eu	Cytokeratin(pan)	C-11	human	BioLegend	628602
17	CD45 154Sm	154Sm	CD45	HI30	human	DVS-Fluidigm	3154001B
18	CD25 155Gd	155Gd	CD25	M-A251	human	BD	555430
19	Vimentin 156Gd	156Gd	Vimentin	RV202	cross	DVS-Fluidigm	3156023A
20	CD324 158Gd	158Gd	CD324 (E-cadherin)	DECMA-1	human	DVS-Fluidigm	3158018B
21	CD11c 159Tb	159Tb	CD11c	Bu15	human	DVS-Fluidigm	3159001B
22	CD279 (PD-1) 160Gd	160Gd	CD279(PD1)	PD1.3.1.3	human	Miltenyi	130-096-168
23	CD152 (CTLA-4) 161Dy	161Dy	CD152(CTLA-4)	14D3	human	DVS-Fluidigm	3161004B
24	FoxP3 162Dy	162Dy	FOXP3	259D/C7	human	DVS-Fluidigm	3162024A
25	CD45RA 163Dy	163Dy	CD45RA	HI100	human	Biolegend	3162024A
26	CD34 164Dy	164Dy	CD34	581	human	BD	555820
27	CD45RO 165Ho	165Ho	CD45RO	UCHL1	human	DVS-Fluidigm	3165011B
28	CD44 166Er	166Er	CD44	BJ18	human	DVS-Fluidigm	3166001B
29	CD38 167Er	167Er	CD38	HIT2	human	BioLegend	303502
30	CD154 (CD40L) 168Er	168Er	CD154 (CD40L)	24-31	human	DVS-Fluidigm	3168006B
31	CD161 169Tm	169Tm	CD161	HP-3G10	human	BioLegend	339902
32	CD3 170Er	170Er	CD3	UCHT1	human	BioLegend	300443

33	CD68 171Yb	171Yb	CD68	Y1/82A	human	DVS-Fluidigm	3171011B
34	CD274 (PD-L1) 172Yb	172Yb	CD274(PD-L1)	29E.2A3	human	Biolegend	3171011B
35	CD14 173Yb	173Yb	CD14	HCD14	human	Biolegend	329702
36	HLA-DR 174Yb	174Yb	HLA-DR	L243	human	Biolegend	325602
37	CXCR4 175Lu	175Lu	CXCR4	12G5	human	DVS-Fluidigm	3175001B
38	Ki67 176Yb	176Yb	Ki67	A019D5	human	BioLegend	3175033B
39	CD16 209Bi	209Bi	CD16	3G8	human	DVS-Fluidigm	3209002B
40	Intercalator-Ir	191Ir	nucleus			DVS-Fluidigm	SKU 201192B
41	Cisplatin-198Pt	198Pt	Cell viability			DVS-Fluidigm	SKU 201198

Supplementary Table 8. IMC antibody panel relevant to Figure 5.

No	PRODUCT	TAG	TARGET	CLONE	reactivity	PRODUCT #
1	CD57 141Pr	141Pr	CD57	NK-1	human	ab212405
2	CD19 142Nd	142Nd	CD19	6OMP31	cross	3142014D
3	Vimentin 143Nd	143Nd	Vimentin	D21H3	cross	3143027D
4	CD326/EpCAM 144Nd	144Nd	CD326 (EpCAM)	9C4	human	3144026D
5	CTLA-4 145Nd	145Nd	CTLA-4		human	A2001
6	NKG2D 146Nd	146Nd	NKG2D	MM0489-10R27	human	ab89807
7	CD163 147Sm	147Sm	CD163	EDHu-1	human	3147021D
8	Pan-Keratin 148Nd	148Nd	Pan-Keratin	C11	human	3148020D
9	CD11b 149Sm	149Sm	CD11b	EPR1344	human/mouse	3149028D
10	IFN-γ 150Nd	150Nd	IFN-γ	B27	human	10761-890
11	CD31 151Eu	151Eu	CD31	EPR3094	human	3151025D
12	CD45 152Sm	152Sm	CD45	CD45-2B11	human	3152016D
13	CD44 153Eu	153Eu	CD44	IM7	human/mouse	3153029D
14	CD11c 154Sm	154Sm	CD11c	Polyclonal	human	3154025D
15	FoxP3 155Gd	155Gd	FoxP3	236A/E7	human	3155016D
16	CD4 156Gd	156Gd	CD4	EPR6855	human	3156033D
17	E-Cadherin 158Gd	158Gd	E-Cadherin	24E10	cross	3158029D
18	CD68 159Tb	159Tb	CD68	KP1	human	3159035D
19	Vista 160Gd	160Gd	Vista	D1L2G	human	3160025D
20	CD20 161Dy	161Dy	CD20	H1	human	3161029D
21	CD8a 162Dy	162Dy	CD8a	C8/144B	human	3162034D
22	PD-L1 163Dy	163Dy	PD-L1		human	conjugated
23	c-Myc p67 164Dy	164Dy	C-Myc p67	9E10	human	3164025D
24	PD-1 165Ho	165Ho	PD-1		human	conjugated
25	CD45RA 166Er	166Er	CD45RA	HI100	human	3166028D
26	Granzyme B 167Er	167Er	Granzyme B	EPR20129-217	human	3167021D
27	Ki-67 168Er	168Er	Ki-67	B56	cross	3168022D
28	MIC 169Er	169Er	MIC	EPR22031	human	ab241513
29	CD3 170Er	170Er	CD3	Polyclonal, C-Terminal	human	3170019D
30	CD27 171Yb	171Yb	CD27	EPR8569	human	3171024D
31	CD161 172Yb	172Yb	CD161	OTI1D8	human	ab273666
32	CD45RO 173Yb	173Yb	CD45RO	UCHL1	human	3173016D
33	HLA-DR 174Yb	174Yb	HLA-DR	YE2/36 HLK	human	3174023D
34	CD25 175Lu	175Lu	CD25	EPR6452	human/mouse	ab213044
35	Lysozyme 176Yb	176Yb	Lyz	EPR2994(2)	human/mouse	ab185129
36	Intercalator-Ir	191Ir	nucleus			SKU 201192B

Supplementary Table 9. CyTOF antibody panel for PBMC, BMMC, and tumor-infiltrating immune cells, relevant to Supplementary Figure 10.

No	PRODUCT	TAG	TARGET	CLONE	reactivity	Source	PRODUCT #
1	CD45 89Y	89Y	CD45	HI30	human	DVS-Fluidigm	3089003B
2	CD57 115In	115In	CD57	HCD57	human	BioLegend	322325
3	IdU I127	127I	S-phase		DNA	Sigma	I7125-5G
4	CXCR2 139La	139La	CD182, CXCR2	5E8	Hu	BioLegend	70785
5	CD49d 141Pr	141Pr	CD49d	9F10	Hu	DVS-Fluidigm	3141004B
6	CD274 142Nd	142Nd	CD274, PD-L1	MIH1	Hu	eBioscience	14-5983-82
7	TIM-3 143Nd	143Nd	TIM3, CD366	BLR033F	Hu	BETHYL	A700-033CF
8	SYB-010 144Nd	144Nd	SYB-010		Hu		
9	CD4 145Nd (MDA)	145Nd	CD4	RPA-T4	Hu, Ch	BioLegend	300502
10	CD8a 146Nd	146Nd	CD8a	RPA-T8	Hu	DVS-Fluidigm	3146001B
11	CD20 147Sm	147Sm	CD20	2H7	Hu	DVS-Fluidigm	3147001B
12	CD27 148Nd	148Nd	CD27	LG.3A10	Hu, Ms, Rt	BioLegend	124202
13	CD279 149Sm	149Sm	CD279, PD-1	EH12.2H7	Hu, Ch, Rh	BioLegend	329902
14	CLA 150Nd	150Nd	CD162, CLA, PSGL-1	HECA-452	Hu, Ms	BD	555946
15	CD14 151Eu	151Eu	CD14	M5E2	Hu	BioLegend	301802
16	TCRgd 152Sm	152Sm	TCRgd	11F2	Hu	DVS-Fluidigm	3152008B
17	CD45RA 153Eu	153Eu	CD45RA	HI100	Hu	DVS-Fluidigm	3153001B
18	Cytokeratin 154Sm	154Sm	Cytokeratin(pan)	C-11	All	BioLegend	628602
19	CD278 155Gd	155Gd	CD278, ICOS	C398.4A	Hu, Ms, Rt, Rh, Sw	BioLegend	313502
20	CD195 (CCR5) 156Gd	156Gd	CD195, CCR5	NP6-G4	Hu	DVS-Fluidigm	3156015A
21	CD25 158Gd	158Gd	CD25	BC96	Hu	BioLegend	302602
22	CCR7(CD197) 159Tb	159Tb	CD197, CCR7	G043H7	Hu, Rh	DVS-Fluidigm	3159003A
23	VISTA 160Gd (Bethyl)	160Gd	VISTA, B7-H5	BLR035F	Hu	BETHYL	A700-035CF
24	CD152 (CTLA-4) 161Dy	161Dy	CD152	14D3	Hu	DVS-Fluidigm	3161004B
25	FoxP3 162Dy	162Dy	FoxP3	259D/C7	Hu, Mk, Rh	DVS-Fluidigm	3162024A
26	CD19 163Dy	163Dy	CD19	HIB19	Hu, Ch	BioLegend	302202
27	CXCR5 164Dy	164Dy	CXCR5, CD185	51505	Hu	DVS-Fluidigm	3164016B
28	CD45RO 165Ho	165Ho	CD45RO	UCHL1	Hu, Cy, Rh, Ch	DVS-Fluidigm	3165011B
29	CD314 166Er	166Er	CD314, NKG2D	ON72	Hu	BC	A08934
30	CXCR7 167Er	167Er	CXCR7	8F11-M16	Hu, Ms	BioLegend	331102
31	CD154 (CD40L) 168Er	168Er	CD154, CD40L	24-31	Hu	DVS-Fluidigm	3168006B
32	CD161 169Tm	169Tm	CD161	HP-3G10	Hu	BioLegend	339902
33	CD3 170Er (MDA)	170Er	CD3	UCHT1	Hu	BioLegend	300443

34	CD68 171Yb	171Yb	CD68	Y1/82A	Hu	DVS-Fluidigm	3171011B
35	CD314 172Yb	172Yb	CD314, NKG2D	1D11	Hu	BioLegend	320802
36	EOMES 173Yb	173Yb	EOMES	644730	Hu	R&D	MAB6166
37	MIC A/B 174Yb	174Yb	MIC A/B, MHC-I	6D4	Hu	DVS-Fluidigm	3174016B
38	CXCR4 175Lu	175Lu	CD184, CXCR4	12G5	Hu, Rh	DVS-Fluidigm	3175001B
39	CD56 176Yb (DVS-NCAM16.2)	176Yb	CD56	NCAM16.2	Hu, Cy, Rh	DVS-Fluidigm	3176008B
40	CD16 209Bi	209Bi	CD16	3G8	Hu, Rh	DVS-Fluidigm	3209002B
41	Intercalator-Ir	191Ir	nucleus			DVS-Fluidigm	SKU 201192B
42	Cisplatin-198Pt	198Pt	Cell viability			DVS-Fluidigm	SKU 201198

Supplementary Figure 1. Consolidated Standards of Reporting Trials (CONSORT) flow diagram.

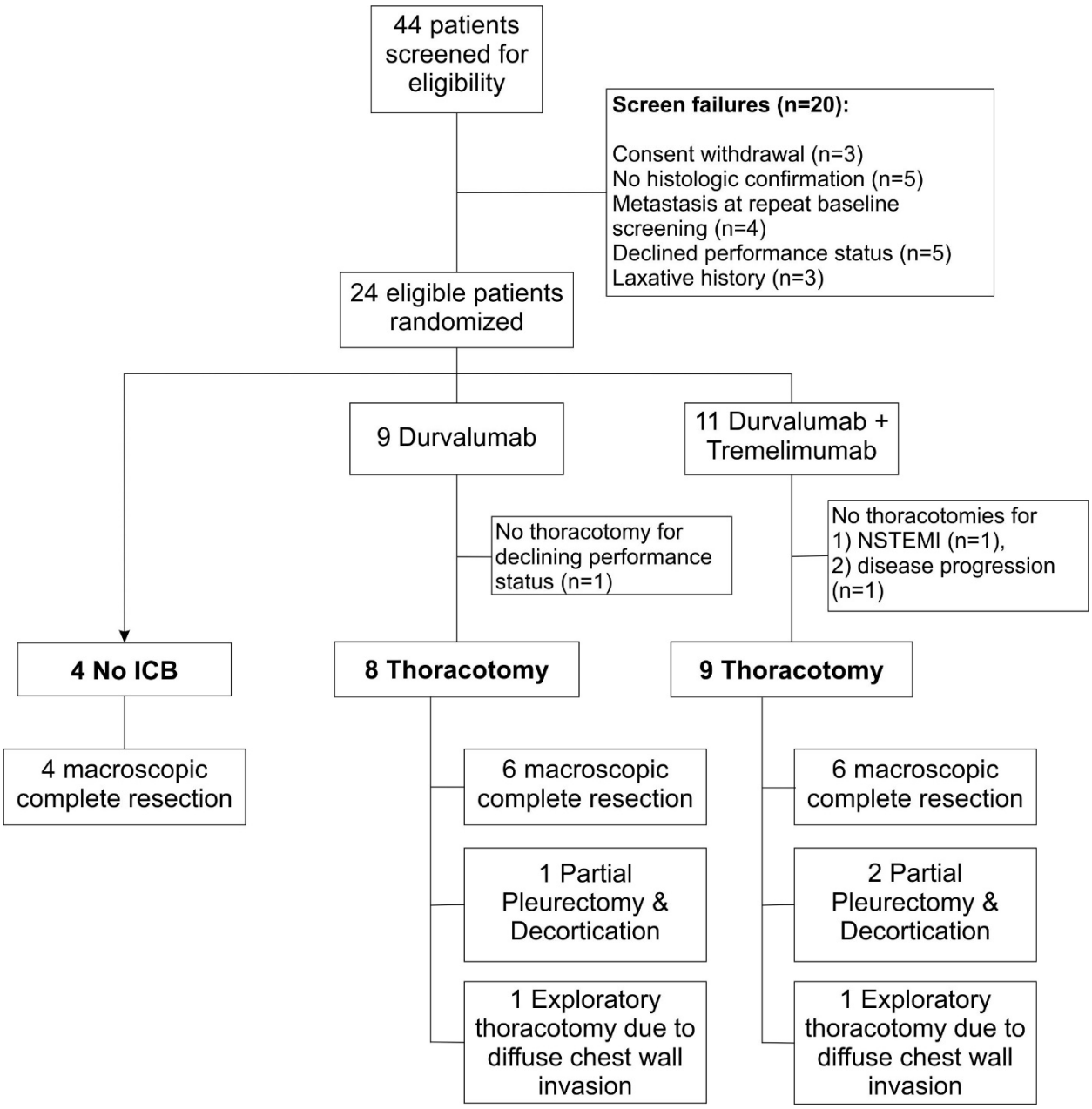

Flow diagram of patient disposition throughout the phases of the study including screening, randomization, neoadjuvant therapy, and surgery.

NSTEMI, non-ST-elevation myocardial infarction.

Supplementary Figure 2. Analysis scheme for imaging mass cytometry (IMC).

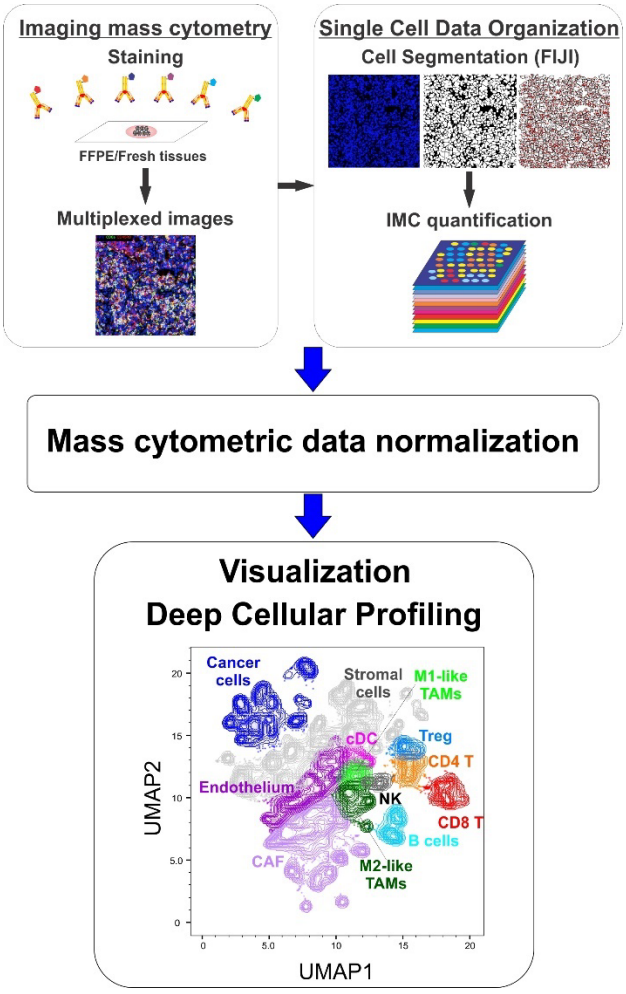

To quantify the .mcd imaging files yielded from imaging mass cytometry (IMC) and to determine the overall spatial architecture of the tumor immune microenvironment, we used the Fiji platform for cell segmentation and conversion of imaging data into flow cytometric data. 32-bit TIFF stacked images were loaded in Fiji and automated cell segmentation was performed by estimating cell boundaries by expanding the perimeter of their nuclei, identified by Cell ID Intercalator-iridium (191Ir). Once images from the IMC methodology are acquired, they were quantified through FIJI's threshold and watershed tools. Protein expression data were then extracted at the single-cell level through mean intensity multiparametric measurements performed on individual

cells, and acquired single-cell data were transferred into additional cytometric analysis in FlowJo® V10 software. All protein markers in quantified IMC data are adjusted with 191Ir and 193Ir nucleus intensities and normalized with CytoNorm across IMC regions of interest (ROIs). CytoNorm is a normalization method for cytometry data applicable to large clinical studies, via a plug-in for FlowJo.

Supplementary Figure 3. Expression of pan-cytokeratin in sarcomatoid malignant pleural mesothelioma.

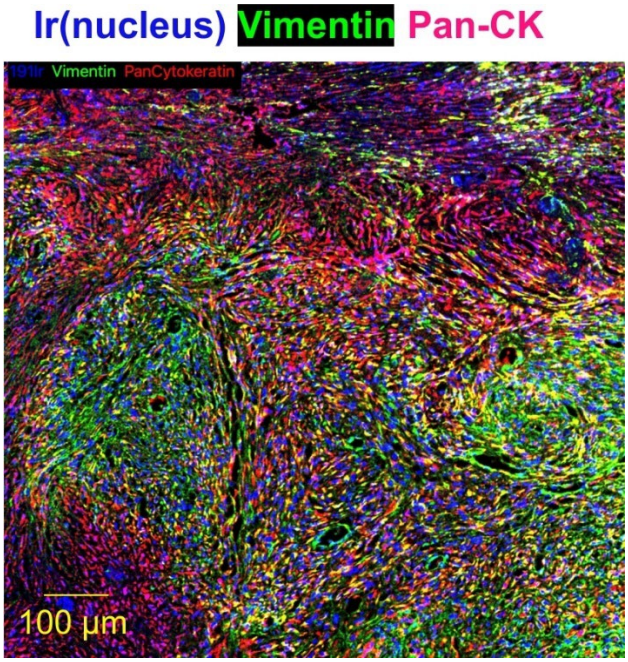

Pan-cytokeratin has proven to be useful in the diagnosis of mesothelioma because virtually all epithelioid MPM and most sarcomatoid MPM produce positive results. In these tumors, aside from immune cells (CD45+PanCK-) and cancer cells regardless of histology (CD45-PanCK+), we demonstrated that cancer-associated fibroblasts (CAF; CD45-PanCK-Vimentin+ cells) and vascular endothelial cells (CD45-PanCK-CD31+ cells) were the main stromal cell types (CD45-PanCK-).

Supplementary Figure 4. Frequencies of other immune and stromal cell compositions before and after ICB.

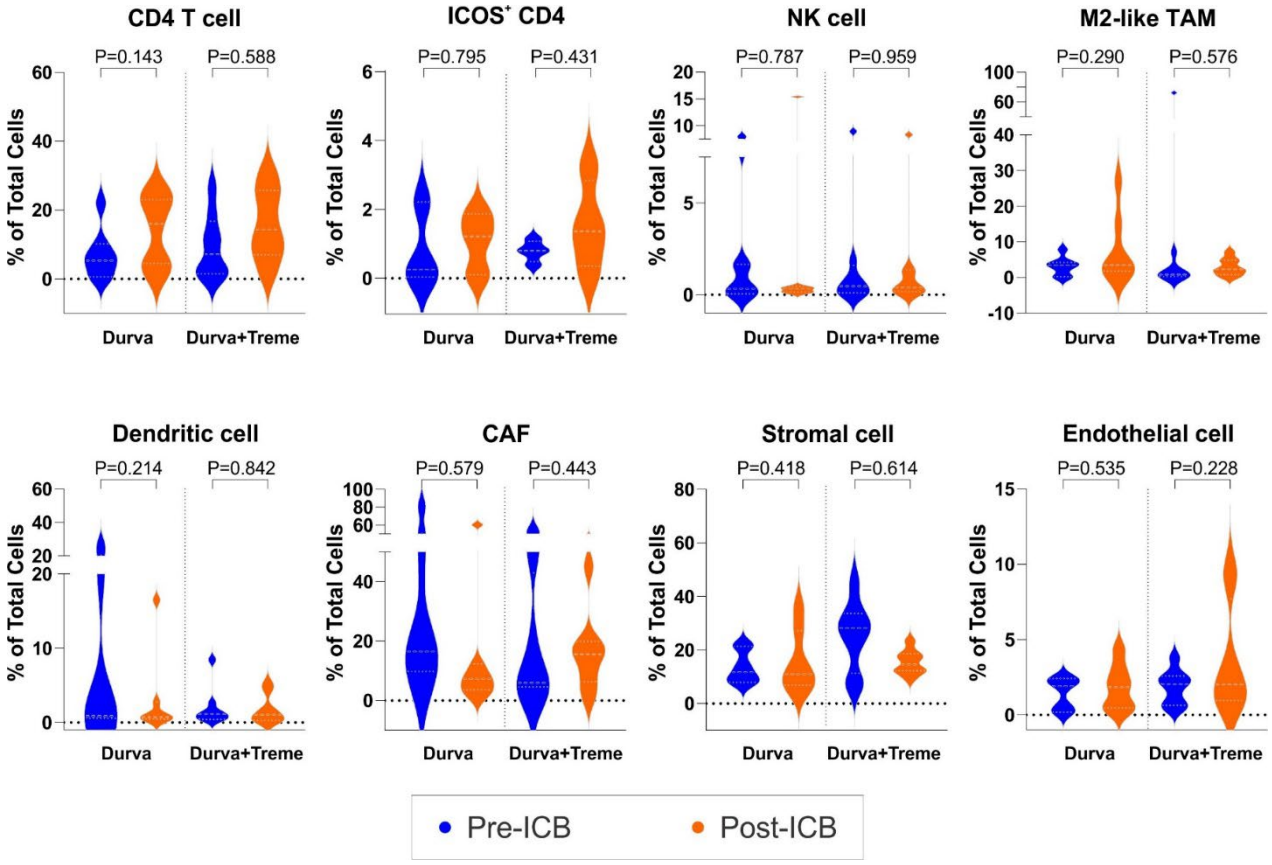

P-values were calculated by paired-t-tests. On each violin plot, the central mark indicates the median, and the bottom and top edges of the plot indicate the 25th and 75th percentiles, respectively.

CAF, cancer-associated fibroblast; ICOS, inducible T cell costimulator; NK, Natural Killer; TAM, tumor-associated macrophage.

Supplementary Figure 5. Overall survival of historical MPM cohorts.

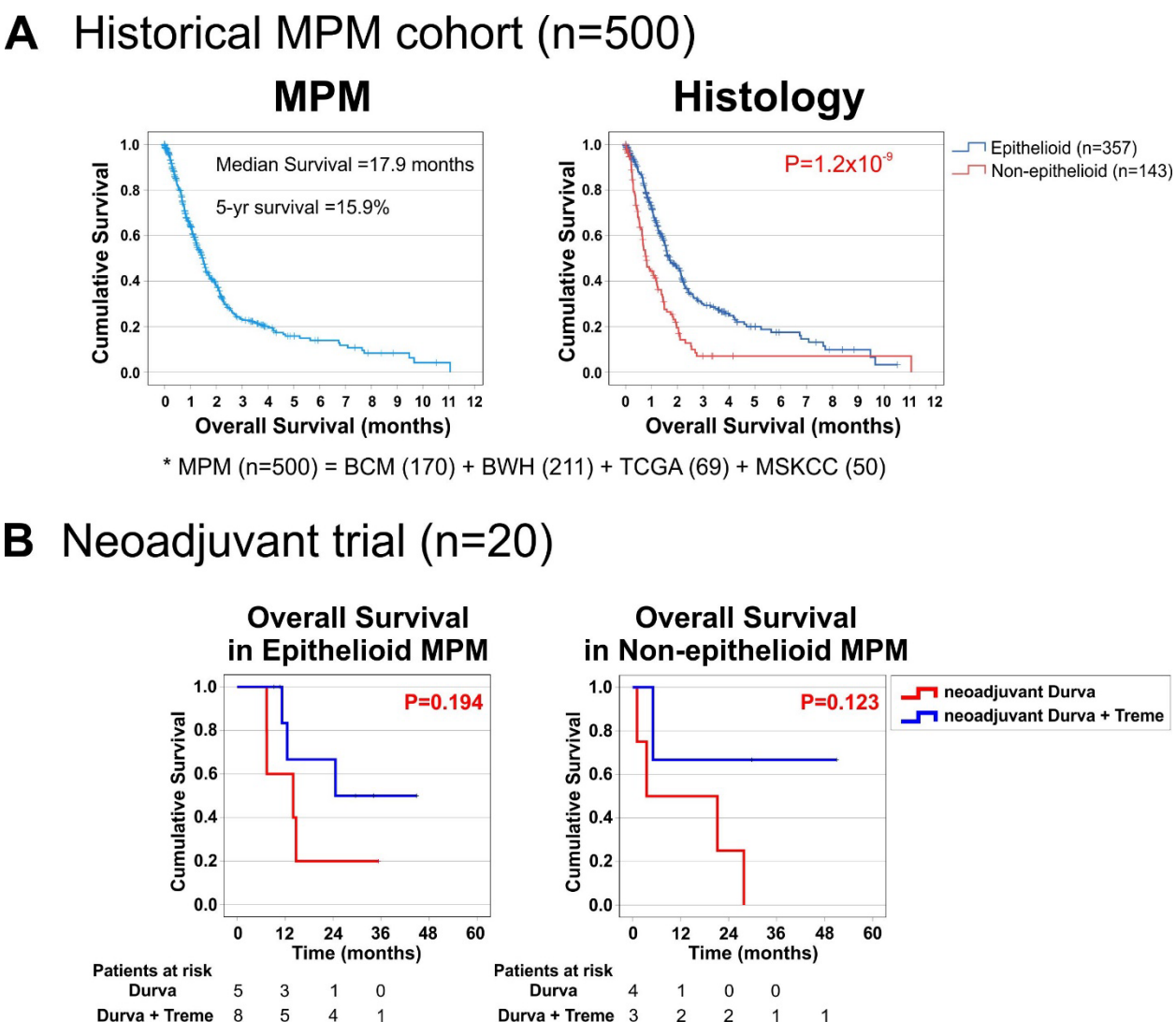

A. Overall survival of historical MPM cohorts. To compare survival data of this study with historical cohorts, we utilized the survival data of 500 MPM patients obtained from the Baylor College of Medicine (BCM) historical cohort (n=170), the Brigham and Women's Hospital (BWH) cohort (n=211), the Cancer Genome Atlas (TCGA) cohort (n=69), and the Memorial Sloan-Kettering Cancer Center (MSKCC) cohort (n=50). **B**. Comparison of overall survival according to the histology in this neoadjuvant clinical trial.

Supplementary Figure 6. Germinal center containing Ki67(+) B cells and CD68(+) fDC-like cell meshwork in mature tertiary lymphoid structure.

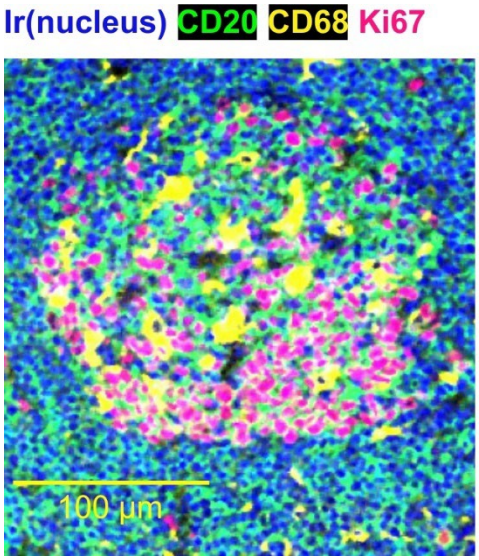

The majority of tertiary lymphoid structures (TLSs) in this study were immature or partially formed TLSs that did not contain a germinal center and a representative TLS shown in **Figure 3A**. As the number of IMC antibodies was limited to 35 to characterize major cell phenotypes, our IMC panel did not include CD21, CD35, or CXCL13 to identify follicular dendritic cells (fDC) in TLSs. Our IMC panel did contain myeloid markers such as CD11b, CD11c, CD68, CD163, and HLA-DR. Herein, we demonstrate presence of a CD68(+) fDC-like cell meshwork in the germinal center of mature TLSs.

Supplementary Figure 7. Characterization of CD57^{+} T cell populations in tumor and PBMCs from MPM patients.

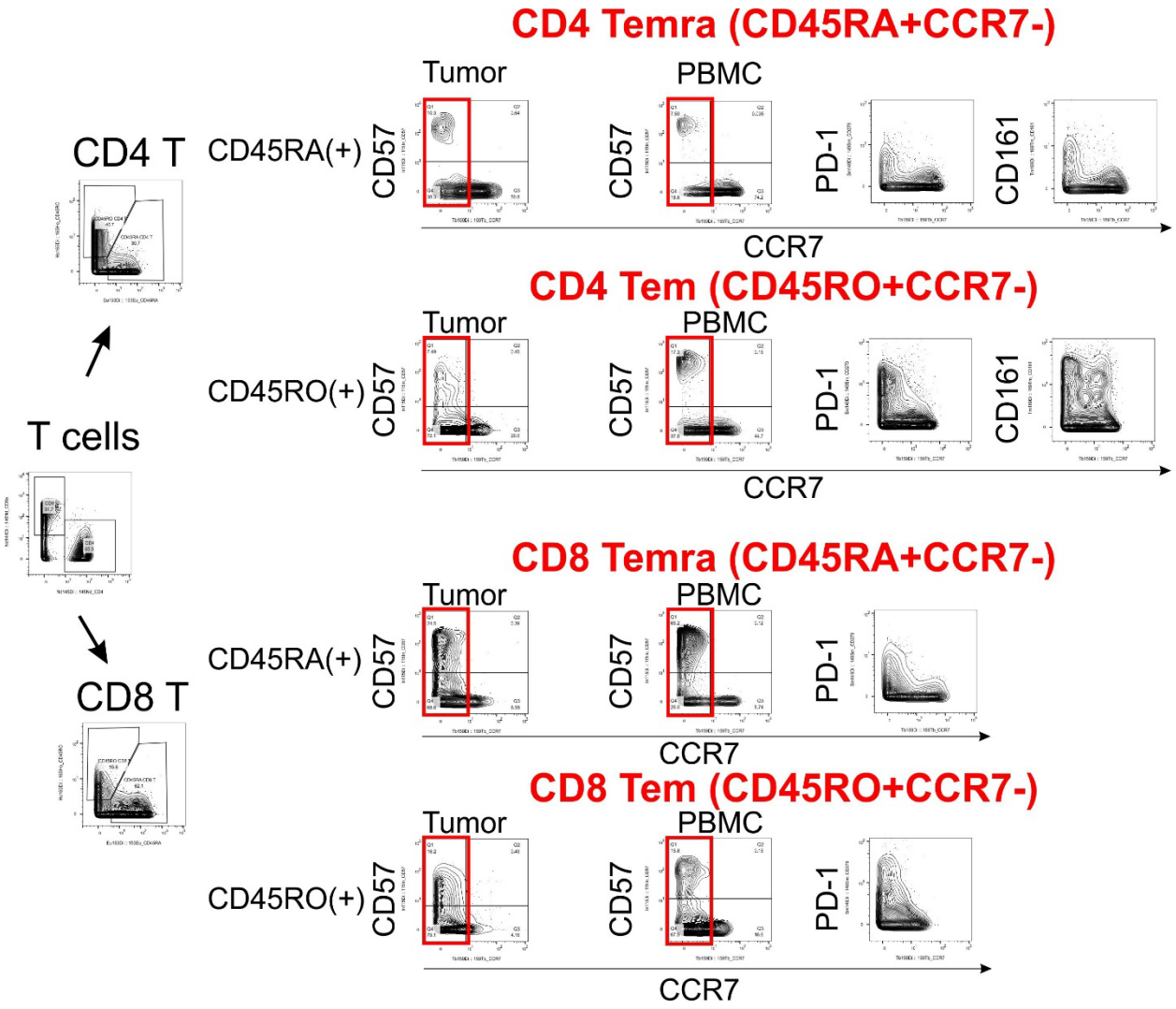

CyTOF analyses demonstrated that CD57^{+} T cells were enriched for CD8 and CD4 effector memory T cells (Tem; CD45^{+}CD3^{+}CD45RO^{+}CD45RA^{-}CCR7^{-}) and CD8 and CD4 effector memory T cells that re-express CD45RA (Temra; CD45^{+}CD3^{+}CD45RA^{+}CD45RO^{-}CCR7^{-}CD27^{-}CD28^{-}). These CD57^{+} T cells had high expression of PD-1.

Supplementary Figure 8. Phenotyping of circulating CD8 and CD4 T cells in MPM patients that received neoadjuvant ICB.

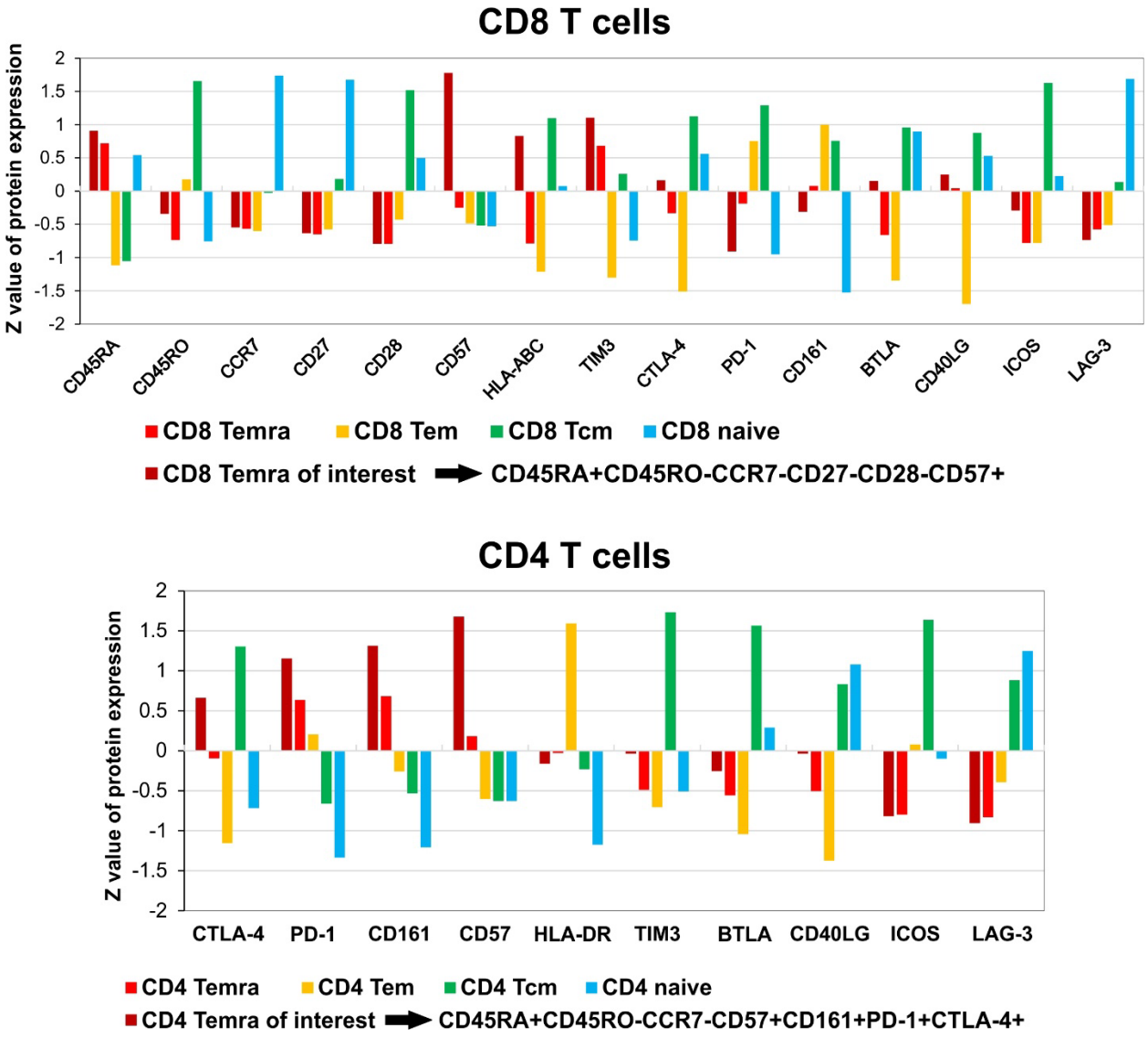

CyTOF revealed that CD57^{+}CD8 Temra was a unique Temra population that overexpressed the immunoregulatory marker TIM-3, and that CD57^{+}CD4 Temra uniquely overexpressed CD161, PD-1, and CTLA-4. CD8 and CD4 "Temra of interest" are the CD57^{+} Temra populations that increased after neoadjuvant durvalumab plus tremelimumab.

Supplementary Figure 9. Alteration of naïve T (Tnaive) and stem cell-like memory T (Tscm) cells in PBMCs and BMMCs.

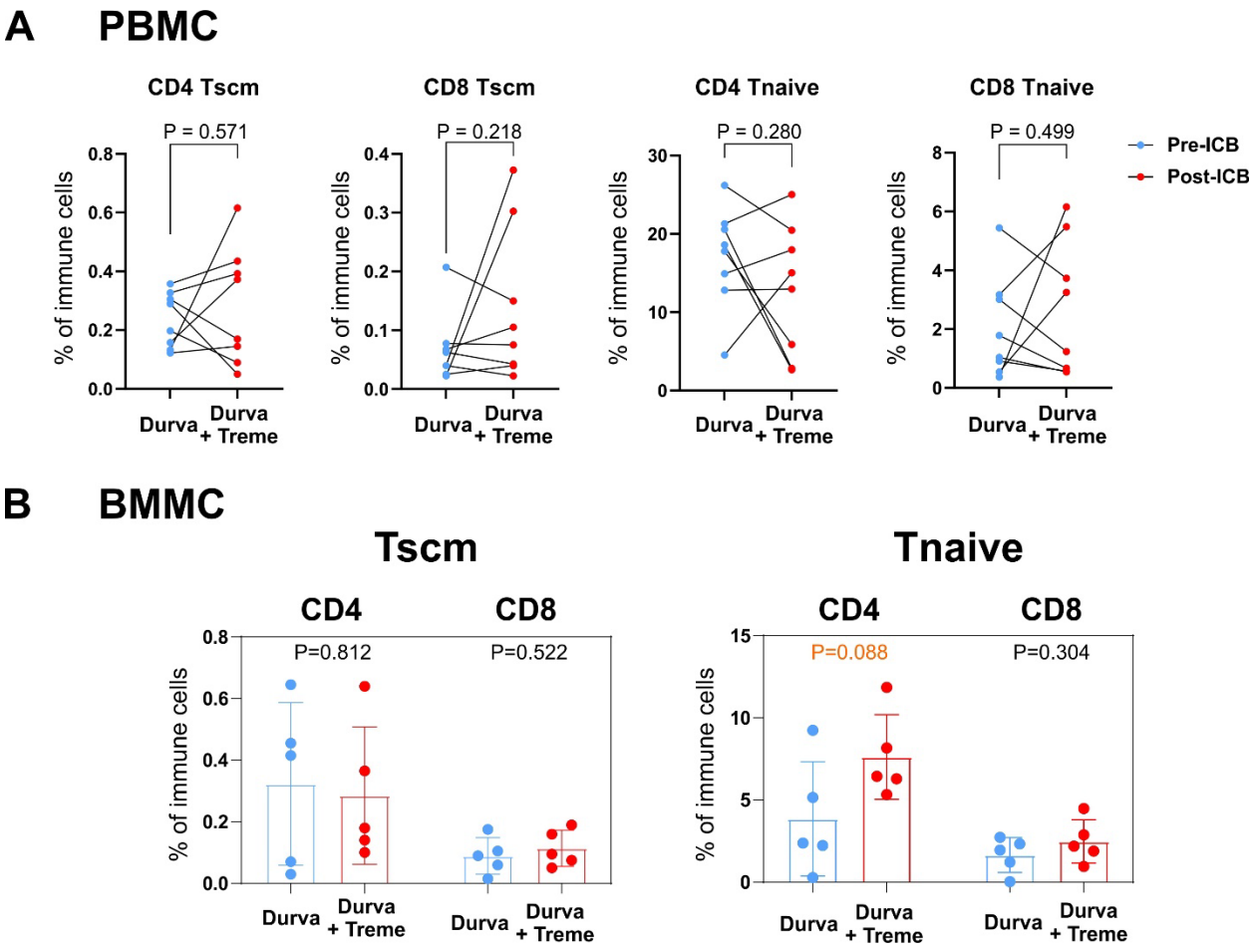

Stem cell–like memory T (Tscm) cells exhibit analogous effector function to memory T cells, but they also have increased proliferation, self-renewal, and strong anti-tumor function compared with conventional memory T cells. Tscm cells share common phenotypic characteristics with naïve T cells as they are CD45+CD3+CD45RA+CD45RO−CCR7+ and CD27+; however, they can be distinguished from naïve T cells by a high expression of CD95, CD122 (IL-2Rβ), and Ki67. We therefore have defined Ki67+ naïve T cells as Tscm. **A**. Tscm and Tnaive cells in PBMCs were not changed during ICB treatment. **B**. Tscm cells in BMMCs were not significantly different between monotherapy and dual therapy. However, CD4 naïve T cells had an increased tendency

after dual ICB treatment, implying that dual ICB may induce T cell differentiation in bone marrow as well as their migration to the tumor-immune microenvironment.

Supplementary Figure 10. Presence of follicular helper T cells in CD57(+) T cells.

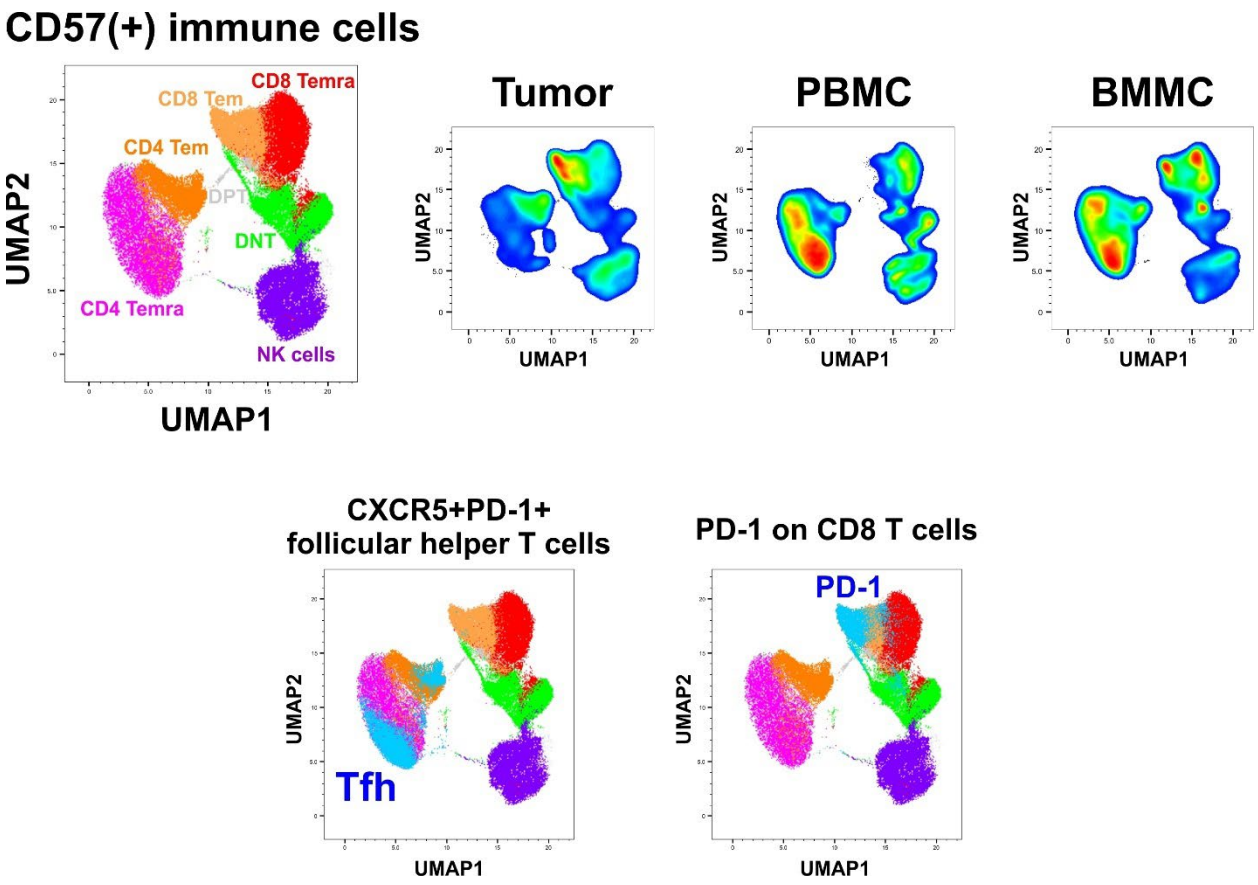

We have characterized CD57(+) immune cells with a CyTOF panel including CXCR5 and PD-1 to confirm the presence of follicular helper T cells in CD57(+) immune cells in the pre-ICB tumor ecosystem, pre-ICB peripheral blood mononuclear cells (PBMCs), post-ICB bone marrow mononuclear cells (BMMCs) because CD57 is not a phenotypic marker for Tfh. CD57(+) cells are mainly composed of 50% CD4 T cells, 21% CD8 T cells, 15% NK cells, and 10% double negative CD4(-)CD8(-)CD3(+) T cells. CD57(+) CD4 T cells consist of 87% CD4 Temra and 10% CD4 Tem, and CD57(+) CD8 T cells consist of 75% CD8 Temra and 21% CD8 Tem. CXCR5(+)PD-1(+) Tfh are 11% in CD4 Temra and 19% of CD4 Tem. CD57(+) CD4 Temra and CD8 Temra were found in pre-ICB tumors, pre-ICB PBMCs, and post-ICB BMMCs. However, CD57(+) CD8 Tem expressing PD-1 was dominant in tumors and post-ICB BMMCs, not in pre-ICB PBMCs.

Supplementary Figure 11. Schematic illustration of the *de novo* anti-tumor immune response to ICB that occurs in the peripheral immune system.

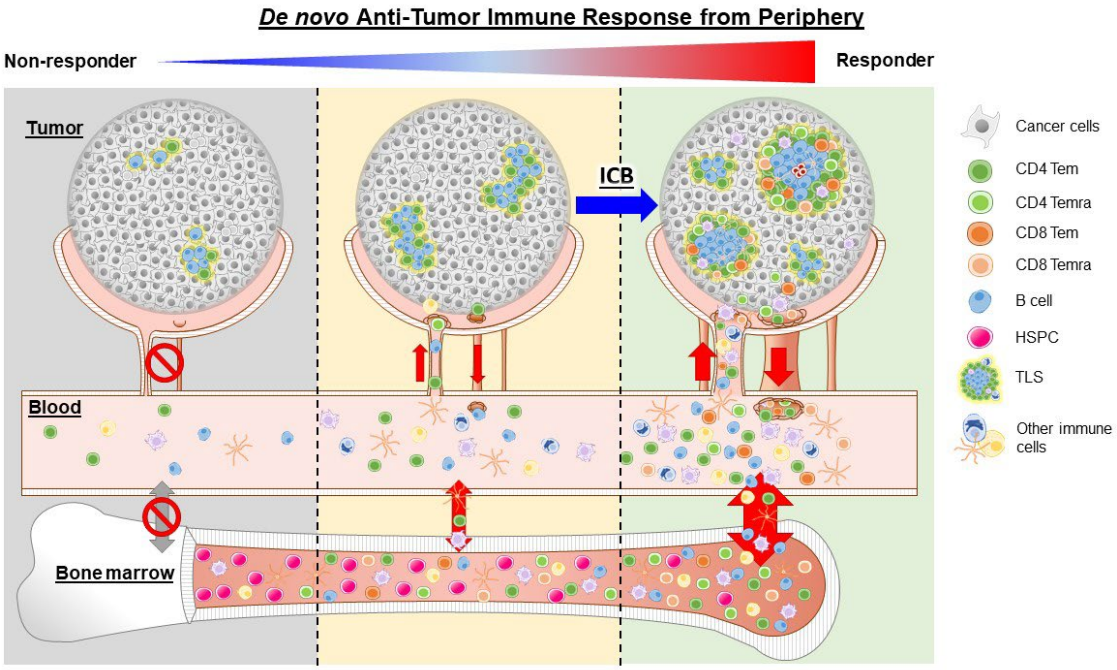

Our data support a paradigm in which effective immune checkpoint blockade generates *de novo* systemic immune responses that originate in the bone marrow and extend to the tumor microenvironment.

SUPPLEMENTARY METHODS

Trial Oversight. The protocol and all modifications were approved by the Institutional Review Board at BCM (H-36952) and all patients provided written informed consent before enrollment. The study was designed and the manuscript was written by authors who vouch for accuracy of its data and adherence to its protocol.

Inclusion Criteria included:

- Written informed consent obtained from the subject prior to performing any protocol-related procedures, including screening evaluations.
- Age greater than 18 years at time of study entry.
- Any MPM histology (epithelial, biphasic, sarcomatoid).
- N0 or N1 nodal disease as present on preoperative chest CT and/or PET-CT.
- Radiographic N2 nodal disease if no progression after 2 cycles of standard chemotherapy.
- Eastern Cooperative Oncology Group (ECOG) performance status of 0 or 1.
- Adequate normal organ and marrow function as defined below: Hemoglobin greater or equal to 9.0 g/dL; Absolute neutrophil count (ANC) greater or equal to 1.5 x 10^9/L (greater than 1500 per mm3); Platelet count greater or equal to 100 x10^9/L (greater than 100,000 per mm3); Serum bilirubin less than or equal to 1.5 x institutional upper limit of normal (ULN); AST (SGOT)/ALT (SGPT) less than or equal to 2.5 x institutional upper limit of normal unless liver metastasis are present, in which case it must be less than or equal to 5 x ULN; Serum creatinine clearance greater than 50 mL/min by the Cockcroft-Gault formula or by 24-hour urine collection for determination of creatinine clearance.

- Female subjects must either be of non-reproductive potential (i.e., post-menopausal by history: greater than or equal to 60 years old and no menses for greater or equal to 1 year without an alternative medical cause; OR history of hysterectomy, OR history of bilateral tubal ligation, OR history of bilateral oophorectomy) or must have a negative serum pregnancy test upon study entry.
- Surgically resectable MPM with no disease extension beyond the ipsilateral hemithorax.
- Planned resectional surgery for MPM by pleurectomy and decortication (P/D) or extrapleural pneumonectomy (EPP).

Exclusion Criteria included:

- Involvement in the planning and/or conduct of the study (applies to both AstraZeneca staff and/or staff at the study site) or previous enrollment or randomization in the present study.
- Participation in another clinical study with an investigational product during the last 3 months.
- Any previous treatment with a PD-1 or PD-L1 inhibitor, including durvalumab.
- Receipt of the last dose of anti-cancer therapy (chemotherapy, immunotherapy, endocrine therapy, targeted therapy, biologic therapy, tumor embolization, monoclonal antibodies, other investigational agent) 30 days prior to the first dose of study drug, and 30 days prior to the first dose of study drug for subjects who have received prior TKIs [e.g., erlotinib, gefitinib and crizotinib] and within 6 weeks for nitrosourea or mitomycin C).
- Current or prior use of immunosuppressive medication within 28 days before the infusion with durvalumab or durvalumab + tremelimumab and through 90 days post infusion, with the exceptions of intranasal and inhaled corticosteroids or systemic corticosteroids at

physiological doses, which are not to exceed 10 mg/day of prednisone, or an equivalent corticosteroid.

- Any unresolved toxicity (greater than CTCAE grade 2) from previous anti-cancer therapy.
- Any prior Grade greater than or equal to 3 immune-related adverse event (irAE) while receiving any previous immunotherapy agent, or any unresolved irAE greater than Grade 1.
- Active or prior documented autoimmune disease within the past 2 years Subjects with vitiligo, Grave's disease, or psoriasis not requiring systemic treatment (within the past 2 years) are not excluded.
- Intraabdominal malignancy discovered at laparoscopy and proven pathologically, or nodal disease discovered at mediastinoscopy (N2 or N3 disease) and proven pathologically.
- N3 nodal disease.
- No tissue obtainable at the time of thoracoscopy.
- Active or prior documented inflammatory bowel disease (e.g., Crohn¿s disease, ulcerative colitis).
- History of primary immunodeficiency.
- History of allogeneic organ transplant.
- History of hypersensitivity to durvalumab.
- History of hypersensitivity to tremelimumab or the combination of durvalumab + tremelimumab.
- Uncontrolled intercurrent illness including, but not limited to, ongoing or active infection, symptomatic congestive heart failure, uncontrolled hypertension, unstable angina pectoris, cardiac arrhythmia, active peptic ulcer disease or gastritis, active bleeding diatheses

including any subject known to have evidence of acute or chronic hepatitis B, hepatitis C or human immunodeficiency virus (HIV).

- Psychiatric illness/social situations that would limit compliance with study requirements or compromise the ability of the subject to give written informed consent.
- Known history of previous clinical diagnosis of tuberculosis.
- History of leptomeningeal carcinomatosis.
- Receipt of live attenuated vaccination within 30 days prior to study entry or within 6 months of receiving durvalumab or durvalumab + tremelimumab.
- Receipt of drugs with laxative properties and herbal or natural remedies for constipation within 90 days of receiving durvalumab or durvalumab + tremelimumab.
- Receipt of sunitinib within 3 months of receiving tremelimumab.
- Female subjects who are pregnant, breastfeeding, or male or female subjects of reproductive potential who are not employing an effective method of birth control.
- Any condition that, in the opinion of the investigator, would interfere with the evaluation of the study treatment or interpretation of subject safety or study results.
- Symptomatic or uncontrolled brain metastases requiring concurrent treatment, inclusive of but not limited to surgery, radiation, and/or corticosteroids.
- Subjects with uncontrolled seizures.
- History of interstitial lung disease/pneumonitis.

Historical MPM groups. To compare survival data of this study with historical cohorts, we utilized the survival data of 500 MPM patients obtained from the Baylor College of Medicine (BCM) historical cohort (n=170),[1, 2] the Brigham and Women's Hospital (BWH) cohort (n=211),[3]

the Cancer Genome Atlas (TCGA) cohort (n=69),[4] and the Memorial Sloan Kettering Cancer Center (MSKCC) cohort (n=50).[5]

Adverse Event Monitoring. Adverse events were monitored for at least 30 days after randomization according to the Common Terminology Criteria for Adverse Events, version 4.03, of the National Institutes of Health.[6]

Evaluation of pathologic response in MPM. Hematoxylin and eosin (H&E)-stained slides of the primary lung tumor and lymph node resection specimens were evaluated and staged according to the AJCC-TNM system, 8th edition.[7, 8] A minimum requirement of 5 sections of the tumor was needed for proper examination of the therapy response, and 3 regions of tumor were examined per case. The histologic parameters used for evaluation of therapy response included those that are used in general for most solid organ tumors including histologic subtype of the tumor, percentage of viable tumor, percentage of necrosis, percentage of fibrosis, dystrophic calcifications, and lymphohistiocytic response surrounding the tumor. Tumor samples from both before and after neoadjuvant ICB were evaluated using these criteria. The tumor bed is defined by residual viable tumor (RVT) + necrosis + regression bed. The total percent surface area(s) of each of these three components is estimated across all slides to calculate immune-related %RVT (%irRVT).

%irRVT = residual viable tumor (RVT) area/total tumor bed area x 100, whereby the total tumor bed = RVT + necrosis + regression bed.

The percentage of tumor regression after ICB was calculated as 100 minus %irRVT. If multiple tumor foci are present, the areas from each are summed such that the %irRVT is a representation of the total primary tumor burden. For the current study, the quantitative immune-

related pathologic response criteria (irPRC)[9] are established as follows: up to 10% residual cancer cells remaining (major pathologic response), > 10% and < 80% residual cancer cells remaining (partial pathologic response), and ≥ 80% residual cancer cells remaining (no pathologic response). This quantification is adopted from non-small cell lung cancer,[8] as there are no published criteria to our knowledge to quantify pathologic complete response in mesothelioma from the previous studies.

PD-L1 Expression & TLS Density. Pre-treatment tumor PD-L1 expression was measured by the FDA-approved PD-L1 clone 28-8 or 22C3 (PharmDx) in FFPE sections and quantified as percentage of tumor cells with membranous PD-L1 staining. The density of tertiary lymphoid structures (TLSs) was calculated as number of TLSs/total area in regions of interest (mm^2).

Assessment of Immunologic Response. Imaging mass cytometry (IMC) was performed on formaldehyde-fixed paraffin-embedded (FFPE) tumor sections using 35 markers (**Supplementary Tables 5 and 8**). Following cell segmentation, data were processed into a single-cell format and plotted by uniform manifold approximation and projection (UMAP) or T-distributed Stochastic Neighbor Embedding (t-SNE)[10, 11] for dimensionality reduction (**Supplementary Figure 2**). Time-of-flight mass cytometry (CyTOF) was performed on peripheral blood mononuclear cells (PBMCs), bone marrow mononuclear cells (BMMCs), and tumor single cells using 42 markers (**Supplementary Tables 6, 7, and 9**) and UMAP was applied to visualize temporal cell trajectories.[12]

Single-cell preparations.

MPM tumors. All human samples were delivered from the operating room to the research laboratory immediately after the specimens were resected. The samples were kept in RPMI without glutamate media in ice during transport. Cancer specimens were processed into single-cell suspensions, fresh frozen tissue preparations, samples cryopreserved in optimal cutting temperature (OCT) compound, and formaldehyde-fixed paraffin-embedded tissues (FFPE). MPM tumors were finely minced and digested in unsupplemented RPMI 1640 (without glutamate) using a human Tumor Dissociation Kit (Miltenyi Biotec Inc., Auburn, CA, USA, Cat.No.130-095-929) in 50 mL Falcon tubes for 30 minutes in the 37°C rotating incubator. Cells were then filtered through a 70 μm cell strainer (Corning Life Sciences Plastic, Cat.No.07201431), washed, and lysed in ACK lysing buffer (Life Technologies, Cat.No.A049201). After centrifuging cells with unsupplemented RPMI media for 5 min at 400g in 20°C and washing two times, supernatants were carefully suctioned off. The cell pellet underwent a final washing with 40 mL supplemented cell culture media (RPMI with FBS), and cells were refiltered through a 70 μm cell strainer. After centrifuging the cells for 5 min at 400g at 20°C, the supernatant was carefully suctioned off. Cells were placed in freezing media (90% FBS with 10% DMSO) and cryopreserved in -80°C freezer storage after cell counting with a cell counter (Countess II FL, Life Technologies, Cat.No.AMQAF1000). For long-term preservation, the cryovials were transferred into a liquid nitrogen tank.

Peripheral blood mononuclear cells (PBMCs) Whole blood was kept in anticoagulant-treated whole blood tubes on ice or at 4°C refrigerators. 15 ml Ficoll-Paque solution was placed into a new 50ml falcon tube. The whole blood was diluted with 15ml DPBS/EDTA (1:1 ratio) and mixed with a pipet. 30 ml of the diluted blood was gently layered on the top of the Ficoll-Paque solution. It was centrifuged for 20 min at 800g, 18°-20°C, without a brake. Plasma samples in the upper

phase were collected, and interphases were collected into a new 50ml falcon tube. After centrifuging cells with DPBS/EDTA solution for 5 min at 300g in 20°C and washing two times, supernatants were carefully suctioned off. Cells were lysed in ACK lysing buffer (Life Technologies, Cat.No.A049201). After centrifuging cells with DPBS for 5 min at 300g in 20°C and washing two times, supernatants were carefully suctioned off. The cell pellet underwent a final washing with 40 mL supplemented cell culture media (RPMI with FBS). After centrifuging the cells for 5 min at 300g at 20°C, the supernatant was carefully suctioned off. Cells were placed in freezing media (90% FBS with 10% DMSO) and cryopreserved in -80°C freezer storage after cell counting with a cell counter (Countess II FL, Life Technologies, Cat.No.AMQAF1000). For long-term preservation, the cryovials were transferred into a liquid nitrogen tank.

Bone marrow mononuclear cells (BMMCs) Resected rib was longitudinally split, and bone marrow was mechanically scraped off. Cells were then filtered through a 70 μm cell strainer (Corning Life Sciences Plastic, Cat.No.07201431), washed, and lysed in ACK lysing buffer (Life Technologies, Cat.No.A049201). After centrifuging cells with unsupplemented RPMI media for 5 min at 400g in 20°C and washing two times, supernatants were carefully suctioned off. The cell pellet underwent a final washing with 40 mL supplemented cell culture media (RPMI with FBS), and cells were refiltered through a 70 μm cell strainer. After centrifuging the cells for 5 min at 400g at 20°C, the supernatant was carefully suctioned off. Cells were placed in freezing media (90% FBS with 10% DMSO) and cryopreserved in -80°C freezer storage after cell counting with a cell counter (Countess II FL, Life Technologies, Cat.No.AMQAF1000). For long-term preservation, the cryovials were transferred into a liquid nitrogen tank.

Imaging mass cytometry (IMC). FFPE tissue samples were sectioned at a 5-μm thickness for IMC. FFPE tissues on charged slides were stained with 1:100 diluted antibody cocktails (concentration of each antibody=0.5mg/mL) as recommended by the user's manual.[13] The slides were scanned in the Hyperion Imaging System (Fluidigm). They were scanned at least four regions of interest in >1mm^2 at 200 Hz. To complex immunological systems such as the tumor microenvironment, pathologist-proven IMC antibodies were stained and analyzed. We investigated the cellular phenotypes and biomarkers of a single tissue sample, observe each components' spatial distribution simultaneously, and compare the qualities of each. This unique and comprehensive analysis of a single tumor sample affords us to draw conclusions between the identification and spatial relationships of the significant cellular components within a tumor microenvironment.

IMC analysis. We require some other image processing and computational methods in order to quantify the .mcd imaging files (Fluidigm) yielded from IMC and to determine the overall spatial architecture of the tumor immune microenvironment.[14] We used the free, open-source, image-analyzing platform Fiji[15, 16] for cell segmentation and conversion of imaging data into flow cytometric data. The advantages offered by Fiji include a fast, robust, unsupervised, automated cell segmentation method requiring minimal expertise in computers. 32-bit TIFF stacked images were loaded in Fiji and we applied our novel method of automated cell segmentation that estimates cell boundaries by expanding the perimeter of their nuclei, identified by Cell ID Intercalator-iridium (191Ir). Once images from the IMC methodology are acquired, they can be quantified through FIJI's threshold and watershed tools. Protein expression data were then extracted at the single-cell level through mean intensity multiparametric measurements performed on individual

cells, and acquired single-cell data were transferred into additional cytometric analysis in FlowJo® V10 software (FlowJo, LLC, OR). All protein markers in quantified IMC data are adjusted with 191Ir and 193Ir nucleus intensities and normalized with CytoNorm[17] across IMC regions of interest (ROIs). CytoNorm is a normalization method for cytometry data applicable to large clinical studies, which is plugged-in FlowJo. CytoNorm allows reducing mass cytometry signal variability across multiple batches of barcoded samples. Normalized IMC data are combined by using FlowJo. Twelve cellular phenotypes in **Figure 1C** were manually defined: cancer cells (CD45-**Pan-cytokeratin(CK)**+E-cadherin+), cancer-associated fibroblasts (CAFs; CD45-Pan-CK-**Vim**+), endothelial cells (**CD31**+), B cells (CD19+**CD20**+CD45RA+), CD4 T cells (CD3+**CD4**+), Treg (CD4+**FoxP3**+), CD8 T cells (CD3+**CD8**+), CD8 memory T cells (CD8mem: CD3+**CD8**+**CD45RO**+), M1-like tumor-associated macrophages (TAMs; **CD68**+**Lysozyme**+CD163-), M2-like TAMs (**CD68**+**CD163**+Lysozyme-), Dendritic cells (**CD11c**+**HLA-DR**+CD3-CD20-), NK cells (**CD16**+CD3-CD20-), and stromal cells (CD45-Pan-CK-Vim-CD31-). Reference phenotypes were generated from quantified IMC data based on representative pathologist-proven IMC markers (bold characters). Pooling of downsampled IMC quantified data (20,000 cells in each sample x 34 samples (4 no ICB and 30 evaluable tumors) = 680,000 cells in **Figure 1**) with reference was used for clustering analysis using FlowJo (**Supplementary Figure 2**).

CyTOF experiments. Single cells were stabilized for 6 hours in media at 37°C. Briefly, 0.5 x 10^6 cells from each sample were barcoded using the Cell-ID 20-Plex Pd Barcoding Kit (Fluidigm, Cat.No. 201060).[18] After washing, cells were resuspended in 1 mL Fix I Buffer (Fluidigm, Cat.No.201065), and incubated for 10 minutes at room temperature (RT). After washing twice

with 1 mL of 1xBarcode Perm Buffer (Fluidigm, Cat.No.201057), each sample was resuspended to be barcoded completely in 800 µL Barcode Perm Buffer. Barcodes were resuspended completely in 100 µL Barcode Perm Buffer and transferred to the appropriate samples. After mixing the sample immediately and completely, the samples were incubated for 30 minutes at RT. After washing twice with 1 mL of Maxpar® Cell Staining Buffer (Fluidigm, Cat.No.201068), the samples were resuspended in 100 µL Maxpar® Cell Staining Buffer, and all barcoded samples were combined into one tube. Cells were washed and incubated with extracellular antibodies for 45 minutes on ice. After overnight at 4°C with resuspension in 1× Fix I buffer, the samples were stained with intracellular antibodies against cells cytokines for 30 minutes at RT and washed. The samples were then stained with intracellular antibodies for 30 minutes at RT and washed. Ten minutes before finishing staining with intracellular antibodies, 0.125 nM Cell-ID^{TM} Intercalator-Ir (Fluidigm®, Cat.No.201192B) in Maxpar® Fix and Perm Buffer (Fluidigm® , Cat.No.201067) was added. After washing cells with PBS and MilliQ water, stained cells were analyzed on a mass cytometer (CyTOF3^{TM} mass cytometer, Fluidigm) at an event rate of 400 to 500 cells per second. All mass cytometry files were normalized together using the mass cytometry data normalization algorithm, which uses the intensity values of a sliding window of these bead standards to correct for instrument fluctuations over time and between samples. The bead standards were prepared immediately before analysis, and the mixture of beads and cells were filtered through a filter cap FACS tubes before analysis. All mass cytometry files were normalized together using the mass cytometry data normalization algorithm,[19] which used the intensity values of a sliding window of these bead standards to correct for instrument fluctuations over time and between samples. Barcodes were deconvoluted using the Debarcoder® software (Fluidigm®).[18, 20]

CyTOF analysis. Total live nucleated cells were used for all analyses and visualized using by T-distributed Stochastic Neighbor Embedding (t-SNE)[10, 11] or Uniform Manifold Approximation and Projection (UMAP) for dimensionality reduction.[12] 20,000 immune cells were downsampled from each sample, and they were integrated into one file after the normalization with CytoNorm.[17] Each phenotype was manually defined in PBMCs and tumor single cells: CD4 T cells (CD45+CD3+CD4+CD8-CD19-), CD8 T cells (CD45+CD3+CD8+CD4-CD19-), double negative T cells (CD45+CD3+CD4-CD8-CD19-), naïve CD4 T cells (CD45+CD3+CD4+CD8-CD19-CD45RA+CD45RO-CCR7+), central memory CD4 T cells (CD4 Tcm: CD45+CD3+CD4+CD8-CD19-CD45RO+CD45RA-CCR7+), effector memory CD4 T cells (CD4 Tem: CD45+CD3+CD4+CD8-CD19-CD45RO+CD45RA-CCR7-), effector memory CD4 T re-expressing CD45RA cells (CD4 Temra: CD45+CD3+CD4+CD8-CD19-CD45RA+CD45RO-CCR7-), naïve CD8 T cells (CD45+CD3+CD8+CD4-CD19-CD45RA+CD45RO-CCR7+), central memory CD8 T cells (CD8 Tcm: CD45+CD3+CD8+CD4-CD19-CD45RO+CD45RA-CCR7+), effector memory CD8 T cells (CD8 Tem: CD45+CD3+CD8+CD4-CD19-CD45RO+CD45RA-CCR7-), effector memory CD8 T reexpressing CD45RA cells (CD8 Temra: CD45+CD3+CD8+CD4-CD19-CD45RA+CD45RO-CCR7-), B cells (CD45+CD19+CD3-), monocytes (CD45+CD3-CD19-HLA-DR+CD14+), tumor-associated macrophages (TAM; CD45+CD3-CD19-HLA-DR+CD68+CD11c-CD123-), conventional DC (CD45+CD3-CD19-HLA-DR+CD14-CD11c+), plasmacytoid dendritic cells (CD45+CD3- CD19-HLA-DR+CD11c-CD123+CD68-), and NK cells (CD45+CD3-CD19-HLA-DR-CD56+).

In BMMCs, each lineage was manually defined: hematopoietic stem and progenitor cells (HSPC: CD34+CD117+Lin-), premature B cells(CD45+CD19+CD20-CD3-), mature B cells

(CD45+CD19+CD20+CD3-), CD4 T cells (CD45+CD3+CD4+CD8-CD19-), CD8 T cells (CD45+CD3+CD8+CD4-CD19-), double-negative T cells (CD45+CD3+CD4-CD8-CD19-), naïve CD4 T cells (CD45+CD3+CD4+CD8-CD19-CD45RA+CD45RO-CCR7+), central memory CD4 T cells (CD4 Tcm: CD45+CD3+CD4+CD8-CD19-CD45RO+CD45RA-CCR7+), effector memory CD4 T cells (CD4 Tem: CD45+CD3+CD4+CD8-CD19-CD45RO+CD45RA-CCR7-), effector memory CD4 T re-expressing CD45RA cells (CD4 Temra: CD45+CD3+CD4+CD8-CD19-CD45RA+CD45RO-CCR7-), naïve CD8 T cells (CD45+CD3+CD8+CD4-CD19-CD45RA+CD45RO-CCR7+), central memory CD8 T cells (CD8 Tcm: CD45+CD3+CD8+CD4-CD19-CD45RO+CD45RA-CCR7+), effector memory CD8 T cells (CD8 Tem: CD45+CD3+CD8+CD4-CD19-CD45RO+CD45RA-CCR7-), effector memory CD8 T re-expressing CD45RA cells (CD8 Temra: CD45+CD3+CD8+CD4-CD19-CD45RA+CD45RO-CCR7-), myeloid cells (CD45+HLA-DR+CD3-CD19-, and NK cells (CD45+CD3-CD19-HLA-DR-CD56+). Given the large quantity of data resulting from the proposed experiments (640,000 cells in **Figure 4A**, 200,000 cells in **Figure 4C**, and 500,000 cells in **Figure 5C**), we used an efficient and comprehensive data analysis pipeline based on the Immune Reference Map framework.[20-22] Mapping of our data onto its interface enabled visualization and precise quantification of immune cells in any sample as a tSNE or UMAP plot, and generation of separate maps for defined groups of patients enables comparison of cellular networks between these groups. To improve efficiency and ease of display of our multiple proposed experiments, we generated the intuitive single-cell maps for each comparison (as in **Figures 1C, 4A, 4C, and 5C**). Cell frequencies or proportions were compared across groups of interest.[20, 23, 24] Based on the outcome of interest, statistically significant changes in cell frequencies for each cluster were shown in a single map with the directionality of change given by color. For deep phenotyping of T cells, Z

values of protein markers were calculated by subtracting average protein expression from raw data for each protein and dividing by its standard deviation. Mean metal intensities (MMI) of proteins were compared between T cells of interest and other representative T cell subpopulations (naïve T, Tcm, Tem, and Temra). Newly identified CD57+ effector memory T cells were validated with flow cytometry gating in **Supplementary Figure 7.**

REFERENCES for Supplementary Information

1. Lee HS, Hamaji M, Palivela N, et al. Prognostic Role of Programmed Cell Death 1 Ligand 1 in Resectable Pleural Mesothelioma. *Ann Thorac Surg* 2021;112:1575-1583.
2. Burt BM, Lee HS, Raghuram AC, et al. Preoperative prediction of unresectability in malignant pleural mesothelioma. *J Thorac Cardiovasc Surg* 2020;159:2512-2520.e2511.
3. Bueno R, Stawiski EW, Goldstein LD, et al. Comprehensive genomic analysis of malignant pleural mesothelioma identifies recurrent mutations, gene fusions and splicing alterations. *Nat Genet* 2016;48:407-416.
4. Hmeljak J, Sanchez-Vega F, Hoadley KA, et al. Integrative Molecular Characterization of Malignant Pleural Mesothelioma. *Cancer Disc* 2018;8:1548-1565.
5. Bott M, Brevet M, Taylor BS, et al. The nuclear deubiquitinase BAP1 is commonly inactivated by somatic mutations and 3p21.1 losses in malignant pleural mesothelioma. *Nat Genet* 2011;43:668-672.
6. Common Terminology Criteria for Adverse Events (CTCAE) (Version 4.03). Common Terminology Criteria for Adverse Events (CTCAE) (Version 4.03),. Available at https://evs.nci.nih.gov/ftp1/CTCAE/CTCAE_4.03/CTCAE_4.03_2010-06-14_QuickReference_8.5x11.pdf.
7. Edition S, Edge S, Byrd D. AJCC cancer staging manual. *AJCC cancer staging manual* 2017.
8. Berzenji L, Van Schil PE, Carp L. The eighth TNM classification for malignant pleural mesothelioma. *Transl Lung Cancer Res* 2018;7:543.
9. Cottrell TR, Thompson ED, Forde PM, et al. Pathologic features of response to neoadjuvant anti-PD-1 in resected non-small-cell lung carcinoma: a proposal for quantitative immune-related pathologic response criteria (irPRC). *Ann Oncol* 2018;29:1853-1860.

10. Amir E-aD, Davis KL, Tadmor MD, et al. viSNE enables visualization of high dimensional single-cell data and reveals phenotypic heterogeneity of leukemia. *Nat Biotechol* 2013;31:545-552.
11. van der Maaten LJP, Hinton GE. Visualizing High-Dimensional Data Using t-SNE. *J Mach Learn Res* 2008;9:2579-2605.
12. Becht E, McInnes L, Healy J, et al. Dimensionality reduction for visualizing single-cell data using UMAP. *Nat Biotechnol* 2018.
13. Jang HJ, Truong CY, Lo EM, et al. Inhibition of CDK4/6 Overcomes Primary Resistance to PD-1 Blockade in Malignant Mesothelioma. *Ann Thorac Surg* 2021;S0003-4975(21)01670-2. doi: 10.1016/j.athoracsur.2021.08.054.
14. Giesen C, Wang HA, Schapiro D, et al. Highly multiplexed imaging of tumor tissues with subcellular resolution by mass cytometry. *Nat Methods* 2014;11:417-422.
15. Schindelin J, Arganda-Carreras I, Frise E, et al. Fiji: an open-source platform for biological-image analysis. *Nat Methods* 2012;9:676-682.
16. Schwendy M, Unger RE, Bonn M, et al. Automated cell segmentation in FIJI® using the DRAQ5 nuclear dye. *BMC bioinformatics* 2019;20:39.
17. Van Gassen S, Gaudilliere B, Angst MS, et al. CytoNorm: A Normalization Algorithm for Cytometry Data. *Cytometry* 2020;97:268-278.
18. Zunder ER, Finck R, Behbehani GK, et al. Palladium-based mass tag cell barcoding with a doublet-filtering scheme and single-cell deconvolution algorithm. *Nat Protoc* 2015;10:316-333.
19. Finck R, Simonds EF, Jager A, et al. Normalization of mass cytometry data with bead standards. *Cytometry* 2013;83:483-494.

20. Lee HS, Jang HJ, Choi JM, et al. Comprehensive immunoproteogenomic analyses of malignant pleural mesothelioma. *JCI insight* 2018;3.
21. Spitzer MH, Gherardini PF, Fragiadakis GK, et al. IMMUNOLOGY. An interactive reference framework for modeling a dynamic immune system. *Science* 2015;349:1259425.
22. Spitzer MH, Carmi Y, Reticker-Flynn NE, et al. Systemic Immunity Is Required for Effective Cancer Immunotherapy. *Cell* 2017;168:487-502 e415.
23. Lee HS, Jang HJ, Shah R, et al. Genomic Analysis of Thymic Epithelial Tumors Identifies Novel Subtypes Associated with Distinct Clinical Features. *Clin Cancer Res* 2017;23:4855-4864.
24. Jang HJ, Lee HS, Ramos D, et al. Transcriptome-based molecular subtyping of non-small cell lung cancer may predict response to immune checkpoint inhibitors. *J Thorac Cardiovasc Surg* 2020;159:1598-1610.e1593.